

# Tests of the electroweak sector with diboson final states at the ATLAS Experiment

*Yee Chinn Yap (DESY) for the ATLAS collaboration  
Lake Louise Winter Institute, 15th February 2019*

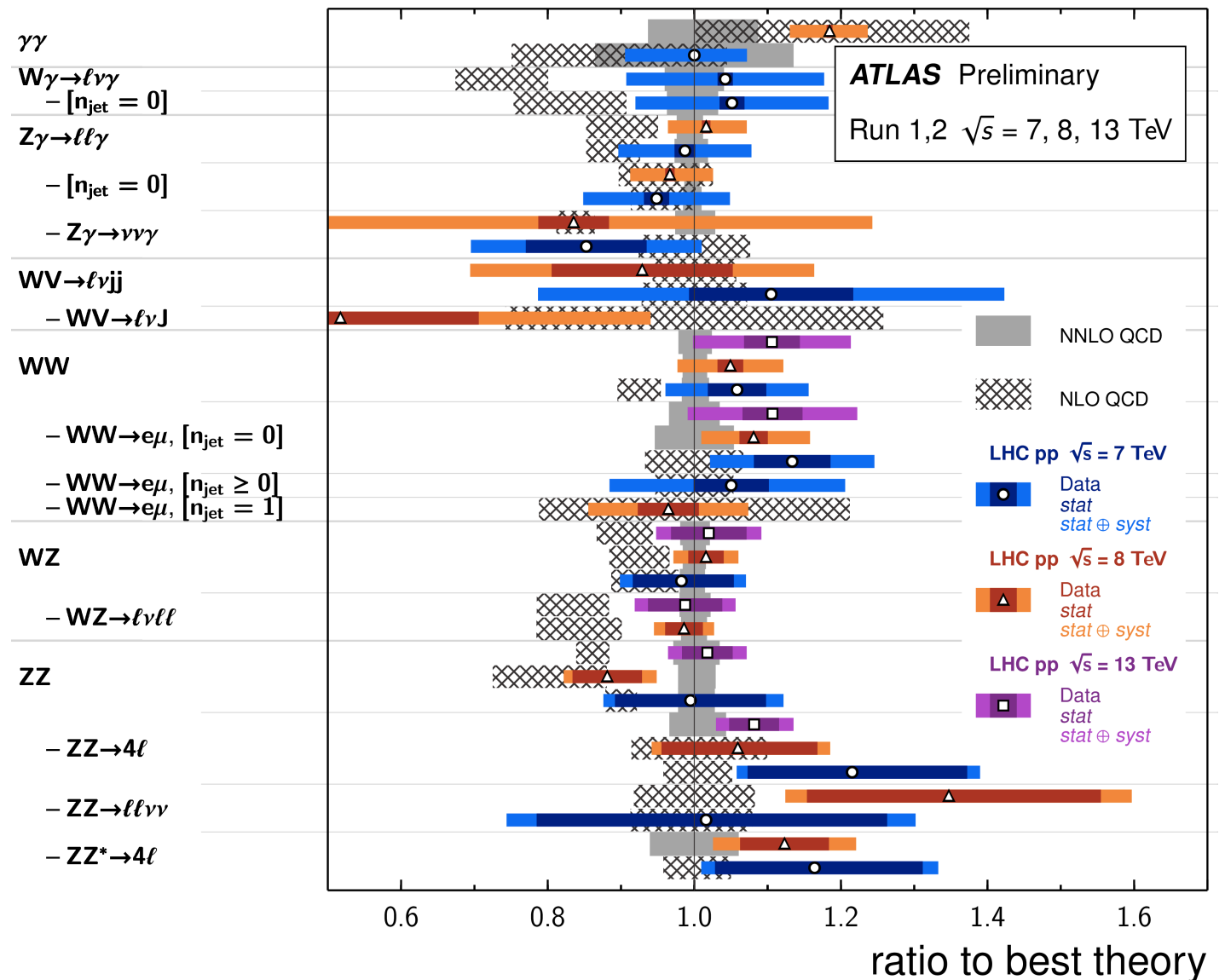


# Introduction

- ❖ Diboson production
  - ❖ Stringent test of the electroweak sector.
  - ❖ Model-independent means to search for new physics at the TeV scale.
- ❖ Vector boson scattering: diboson production in association with two jets.
- ❖ Key process to investigate electroweak symmetry breaking.

Diboson Cross Section Measurements

Status: July 2017



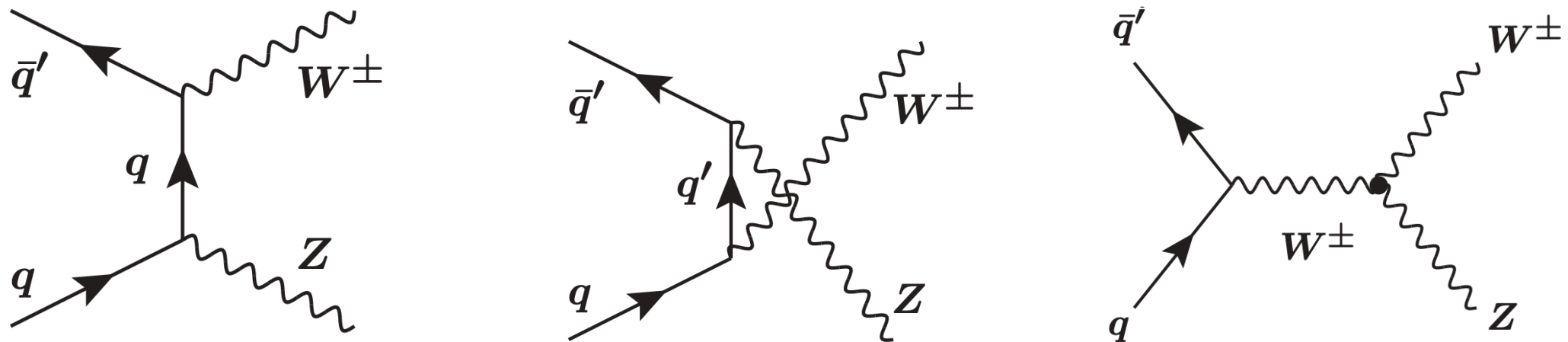
---

# Overview

---

- ❖ In this talk I'll cover three analyses using  $36.1 \text{ fb}^{-1}$  of  $pp$  collision data recorded in 2015 and 2016 at  $\sqrt{s}=13 \text{ TeV}$ :
  - ❖ Measurement of  $W^{\pm}Z$  production cross sections and gauge boson polarisation ATLAS-CONF-2018-034 **Paper submitted to EPJC today, will appear on arXiv on Monday STDm-2018-03**
  - ❖ Observation of electroweak production of  $W^{\pm}Z$  boson pair in association with two jets arXiv:1812.09740 [hep-ex]
  - ❖ Observation of electroweak production of a same-sign  $W$  boson pair in association with two jets ATLAS-CONF-2018-030
- ❖ New diboson results not covered:
  - ❖ Measurement of  $Z\gamma \rightarrow \nu\nu\gamma$  cross-sections and limits on anomalous triple gauge-boson couplings JHEP 12 (2018) 010

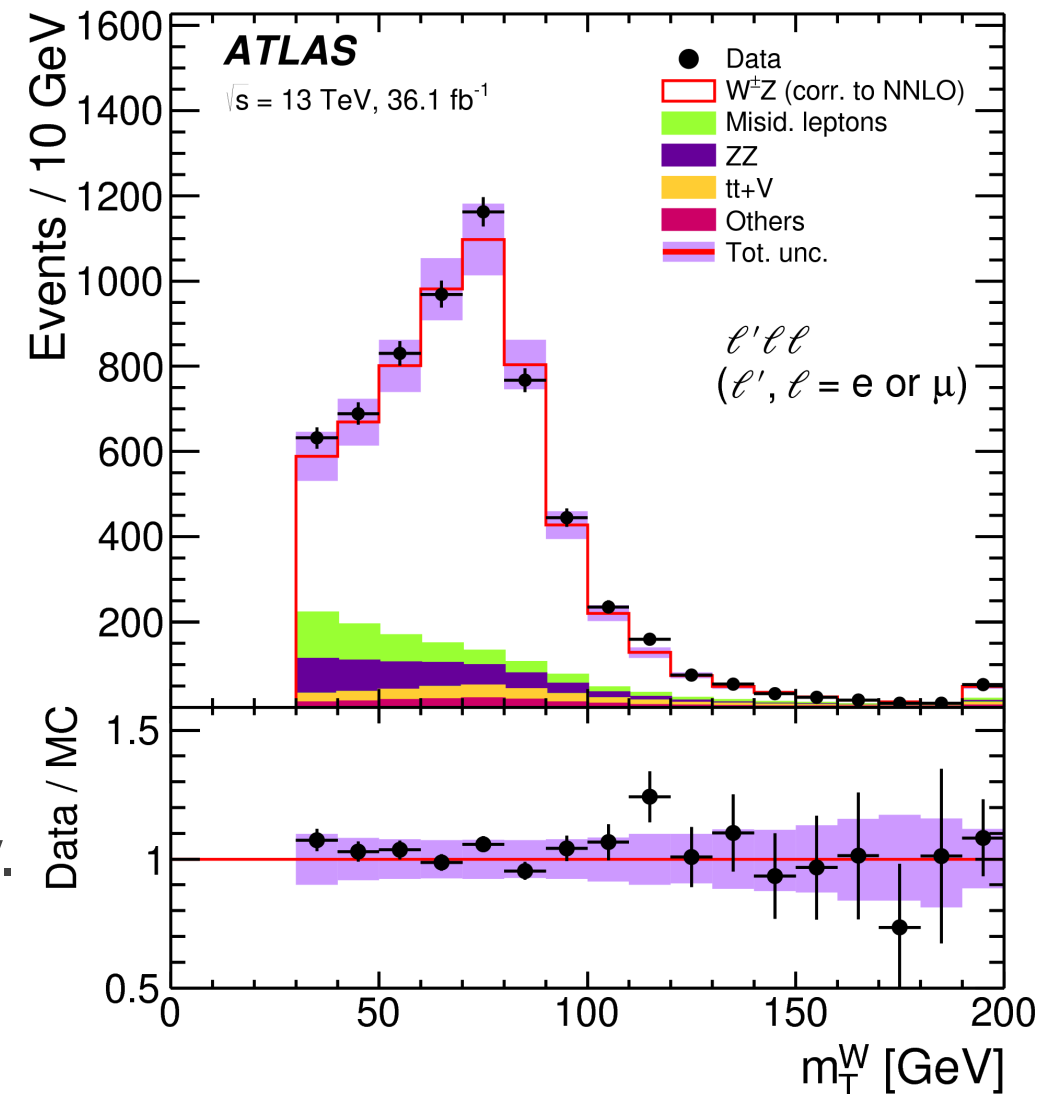
# $W^\pm Z$ production



- ❖ Use leptonic (e, mu) decay modes of the gauge bosons.
- ❖ 3 isolated well reconstructed e and  $\mu$ , veto fourth lepton to suppress ZZ.
- ❖ Fiducial phase space:
  - ❖  $Z \rightarrow \ell\ell$ :  $p_T^\ell > 15$  GeV,  $|\eta| < 2.5$ ,  $|\cos\theta_{\ell\ell} - \cos\theta_Z| < 10$  GeV.
  - ❖  $W \rightarrow \ell\nu$ :  $p_T^{\ell\nu} > 20$  GeV,  $|\eta| < 2.5$ , transverse mass  $m_T^W > 30$  GeV.
  - ❖  $\Delta R(\ell, \ell') > 0.3$ ,  $\Delta R(\ell, \ell) > 0.2$ .
  - ❖ Anti- $k_T$  with  $R=0.4$  particle-level jets:  $p_T > 25$  GeV and  $|\eta| < 4.5$ .

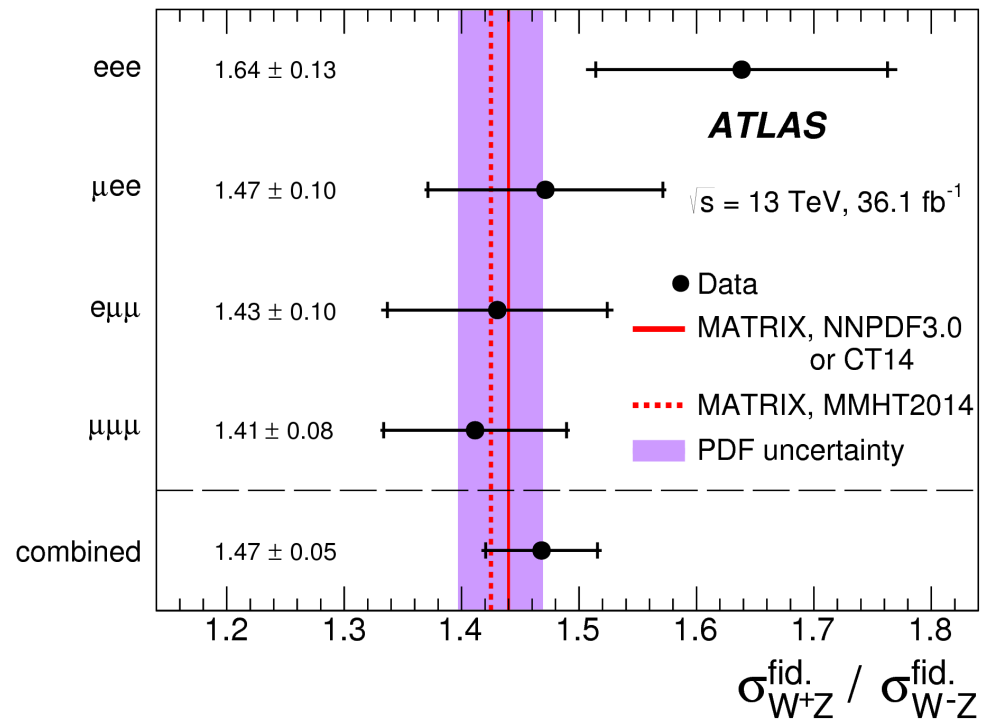
# $W^{\pm}Z$ production

- ❖ Signal: generated with Powheg-Box at NLO in QCD, shower with Pythia 8.210
- ❖ Background:
  - ❖ Reducible: Fake lepton (measured in data)
  - ❖ Irreducible: ZZ, ttV, tZ, VVV (MC normalised to data CR)
- ❖ Systematics: dominated by the uncertainty on reducible background, followed by luminosity.



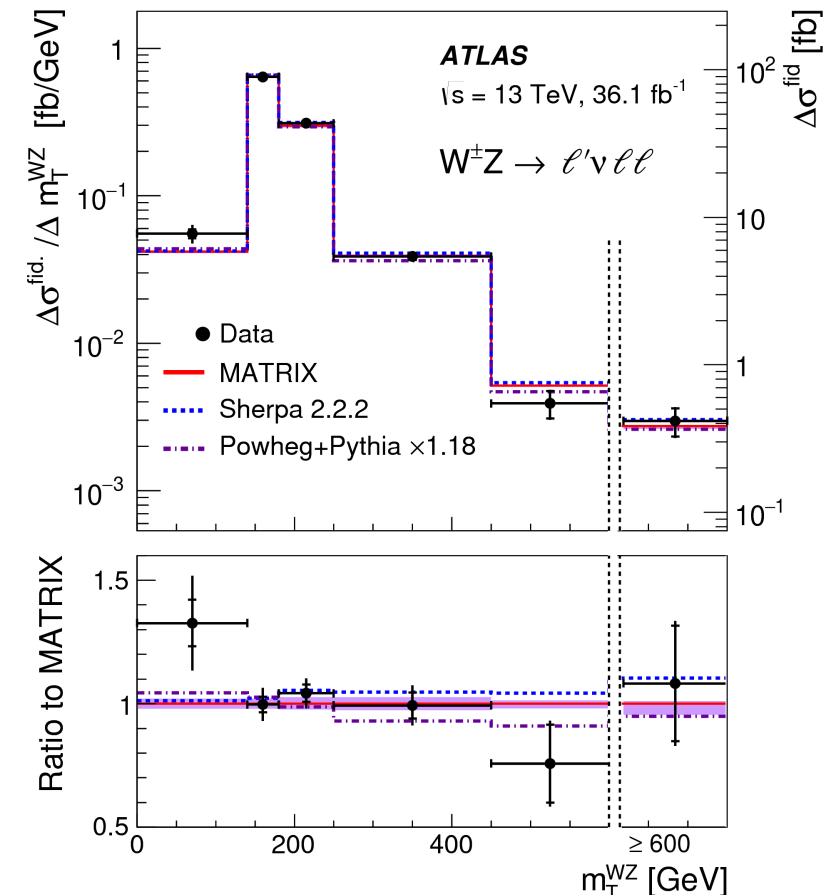
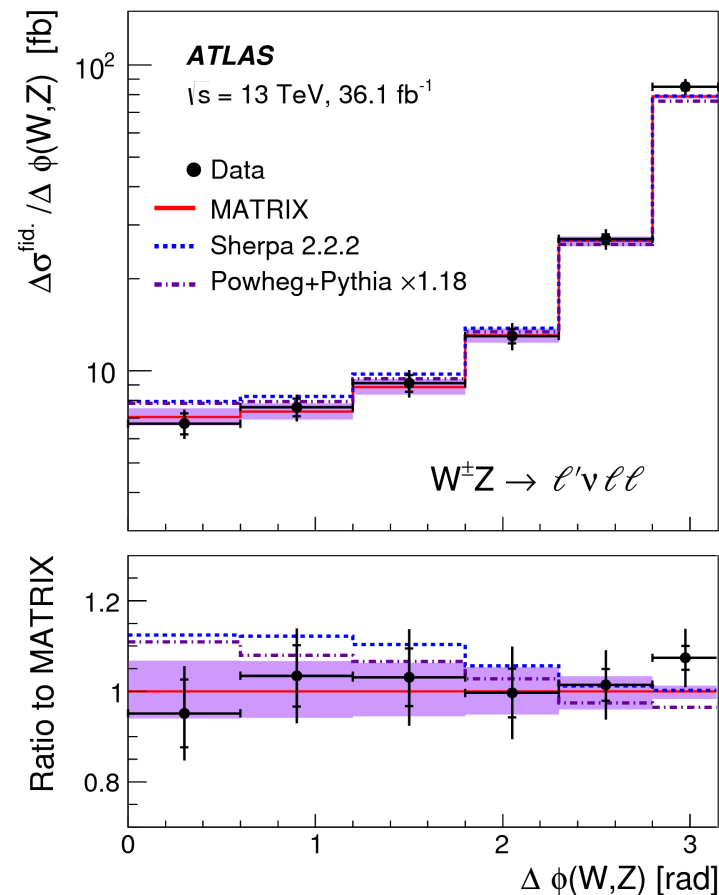
- ❖  $\sigma^{\text{fid.}}_{W^{\pm}Z \rightarrow l' \nu l l} = 63.7 \pm 1.0 \text{ (stat.)} \pm 2.3 \text{ (sys.)} \pm 0.3 \text{ (mod.)} \pm 1.5 \text{ (lumi.) fb}$
- ❖ NNLO prediction (MATRIX):  $61.5^{+1.4}_{-1.3} \text{ fb}$

# $W^\pm Z$ cross-sections



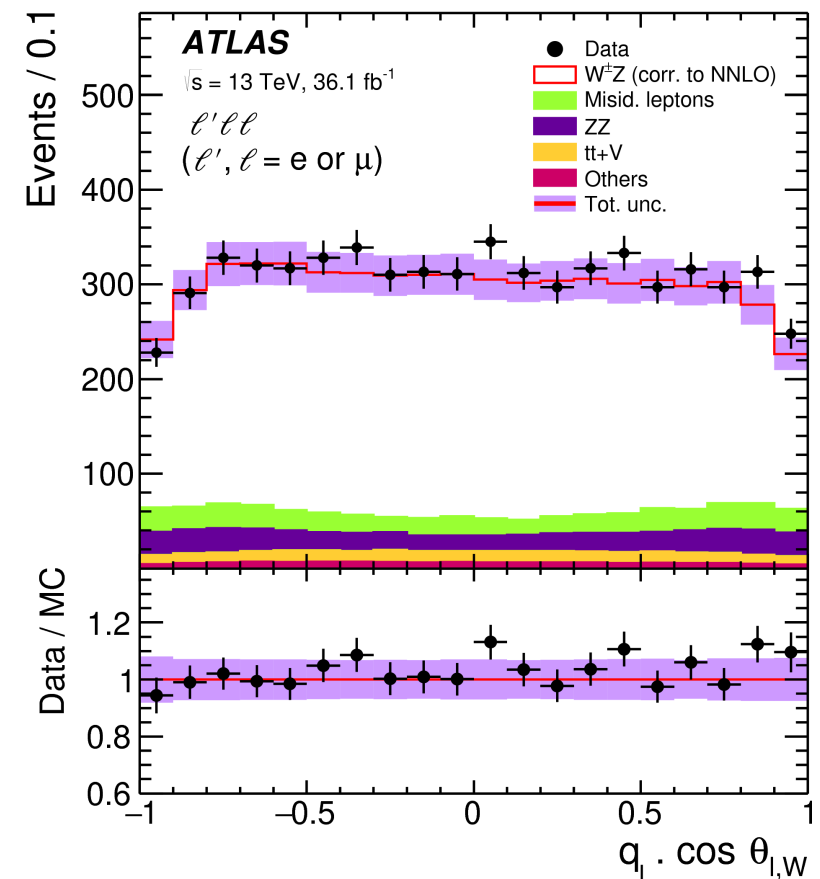
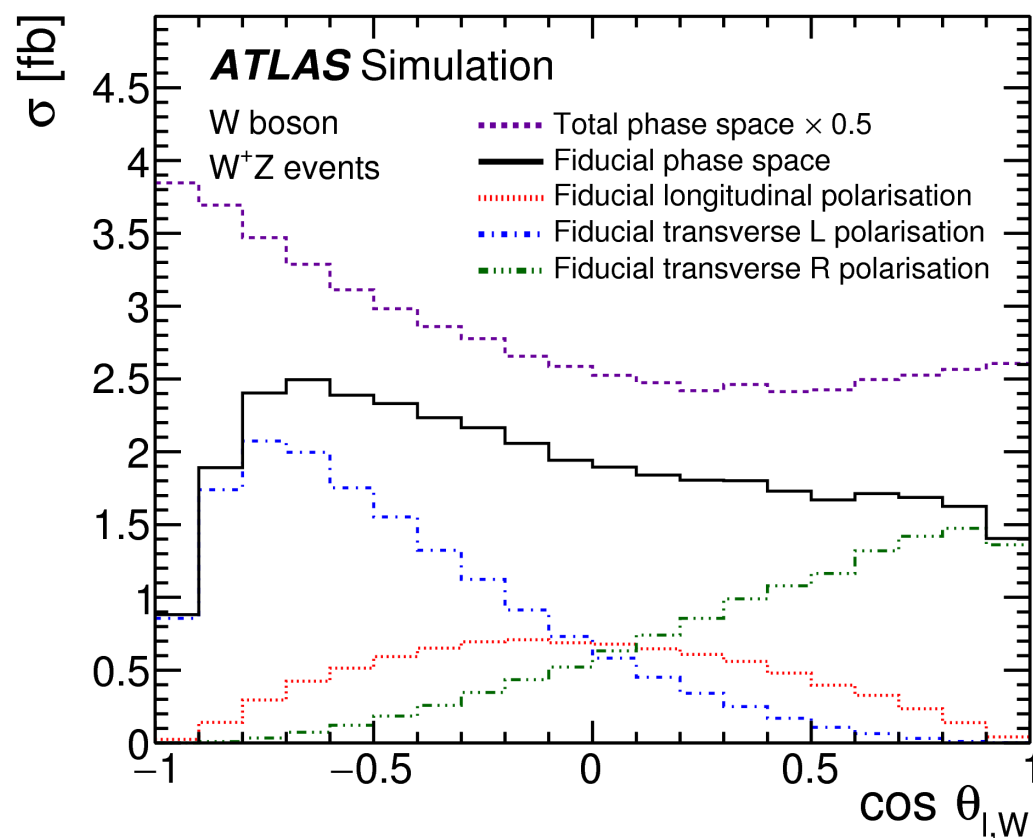
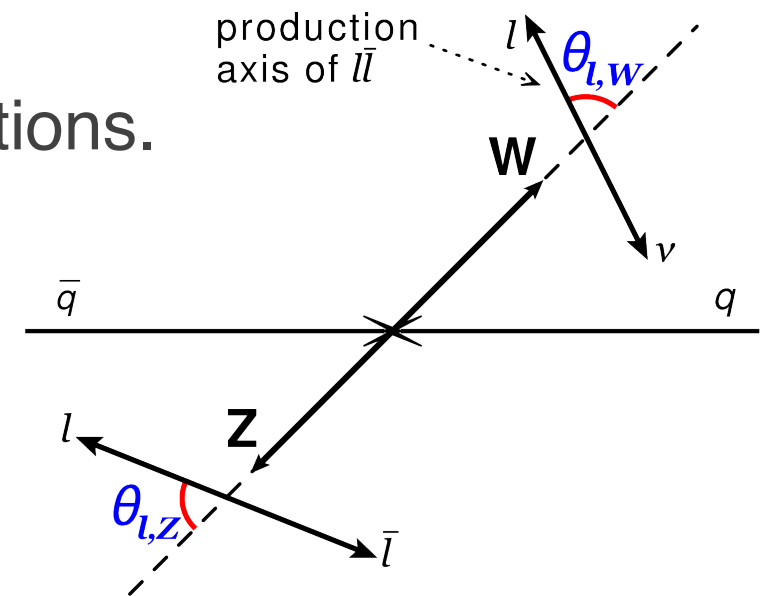
- ❖ Ratio of the  $W^+Z/W^-Z$  cross sections, which is sensitive to the PDF is also measured.
- ❖ Most systematics cancelled in the ratio.

- ❖ Differential cross sections for  $p_T^Z, p_T^W, m_T^{WZ}, \Delta\phi(W, Z), p_T^\nu, |y_Z - y_{l,W}|, N_{jets}, m_{jj}$



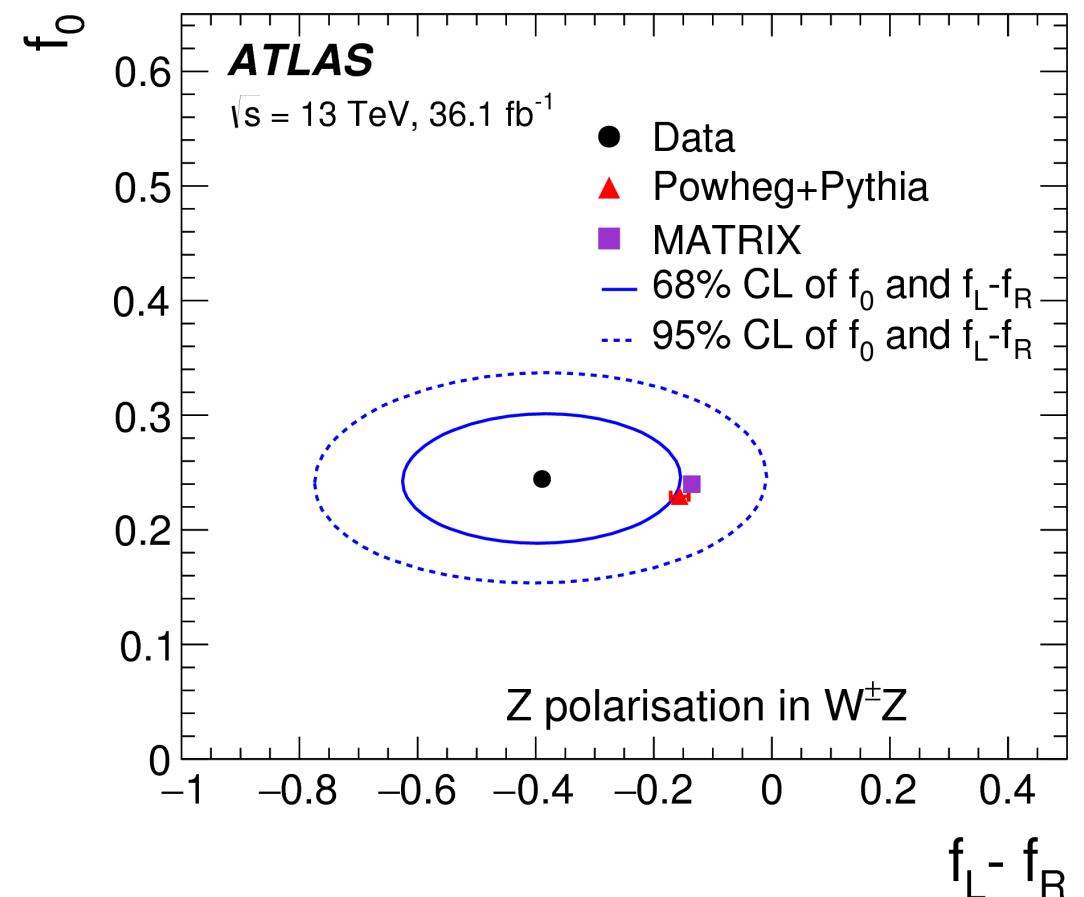
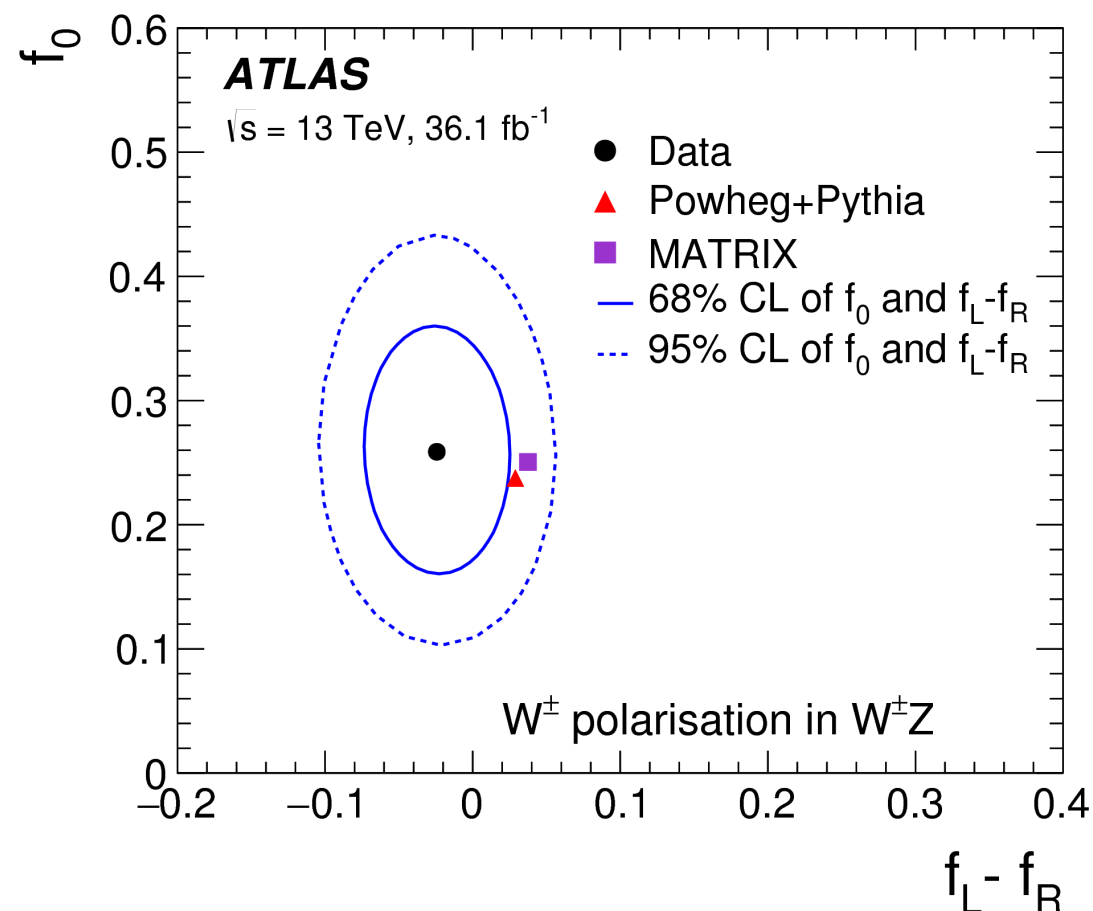
# $W^\pm/Z$ polarisation

- ❖ Measure  $W/Z$  polarisation using lepton angular distributions.
- ❖ Helicity parameters measured using template fit of  $q_\ell \cdot \cos \theta_{\ell,W}$  and  $\cos \theta_{\ell,Z}$  distributions.
- ❖  $m_W$  constraint to solve for neutrino longitudinal momentum at detector level.



# $W^\pm/Z$ polarisation

- ❖ Obs. (exp.) significance of  $4.2\sigma$  ( $3.8\sigma$ ) for longitudinally polarised W bosons.
- ❖  $f_0, f_L, f_R$ : longitudinal, transverse left-handed, transverse right-handed helicity fractions.  $f_0 + f_L + f_R = 1$ .
- ❖ Both MATRIX and Powheg is LO in EW coupling.



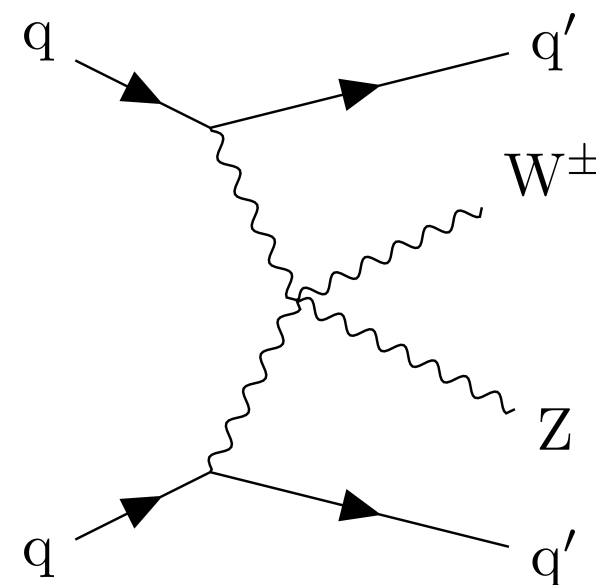
# Vector boson scattering

- ❖ VBS process is an important test of the electroweak sector.
  - ❖ Higgs boson restores unitarity in scattering amplitude.
  - ❖ Sensitive to quartic gauge couplings.
- ❖ All EW-induced processes (only EW interaction vertices) treated as signal, QCD-induced (at least one strong interaction vertex) as background.

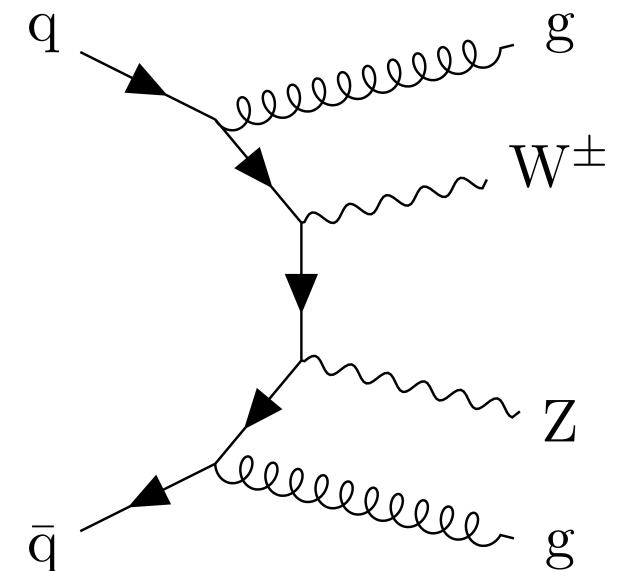
- ❖ QCD-induced background dominant (except in same-sign WW).

- ❖ VVjj EW and QCD-induced processes interfere.

**EW production  $\mathcal{O}(\alpha^4)$**



**QCD-induced production  $\mathcal{O}(\alpha^2\alpha_s^2)$**



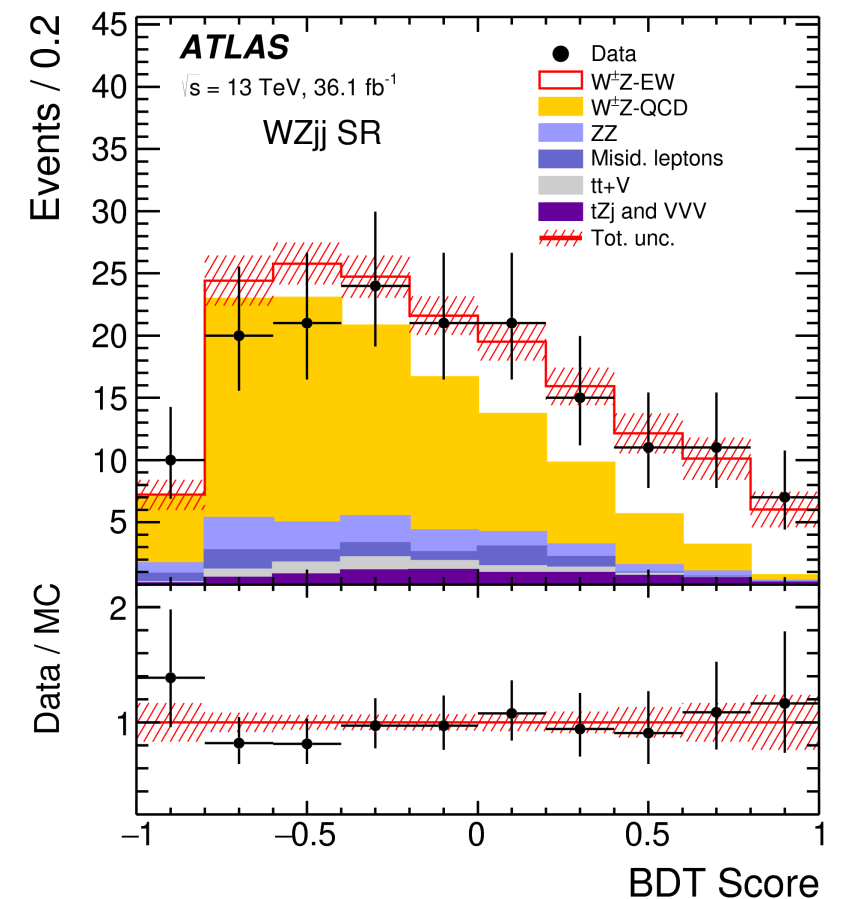
# Vector boson scattering

- ❖ Typical topology:
  - ❖ 2 high energy jets with wide rapidity separation and large  $m_{jj}$ .
  - ❖ Hadronic activity suppressed between the two jets.
  - ❖ Boson pair more central than in non-EWK processes.
- ❖ ATLAS VBS measurements:

Process	Remarks	$\sqrt{s}$	L	Reference
$W^\pm W^\pm$	<b>this talk</b>	13 TeV	36.1 fb <sup>-1</sup>	<a href="#"><u>ATLAS-CONF-2018-030</u></a>
$W^\pm Z$	<b>this talk</b>	13 TeV	36.1 fb <sup>-1</sup>	<a href="#"><u>arXiv:1812.09740 [hep-ex]</u></a>
$Z\gamma$	2 $\sigma$ significance, cross-sections, aQGC limits	8 TeV	20.2 fb <sup>-1</sup>	<a href="#"><u>JHEP07(2017)107</u></a>
Semi leptonic $WW/WZ$	aQGC limits	8 TeV	20.2 fb <sup>-1</sup>	<a href="#"><u>Phys. Rev. D 95 (2017) 032001</u></a>

# WZ VBS

- ❖ Fiducial phase-space: similar to the WZ measurement already discussed.
- ❖ Additionally, 2 jets with  $p_T > 40$  GeV,  $|\eta| < 4.5$ ,  $\Delta R(j,l) > 0.3$ ,  $m_{jj} > 500$  GeV, b-jet veto.
- ❖ Signal: Sherpa 2.2.2 WZjj
- ❖ Background: largest is QCD WZjj (from Sherpa, normalised to data in CR), ZZ, ttV and reducible background.
- ❖ Signal purity  $\sim 13\%$ .
- ❖ Boosted decision tree used to separate signal from background. (15 input variables based on jet, vector boson and lepton kinematics)
- ❖ Systematics: jet energy scale dominant, followed by modelling.



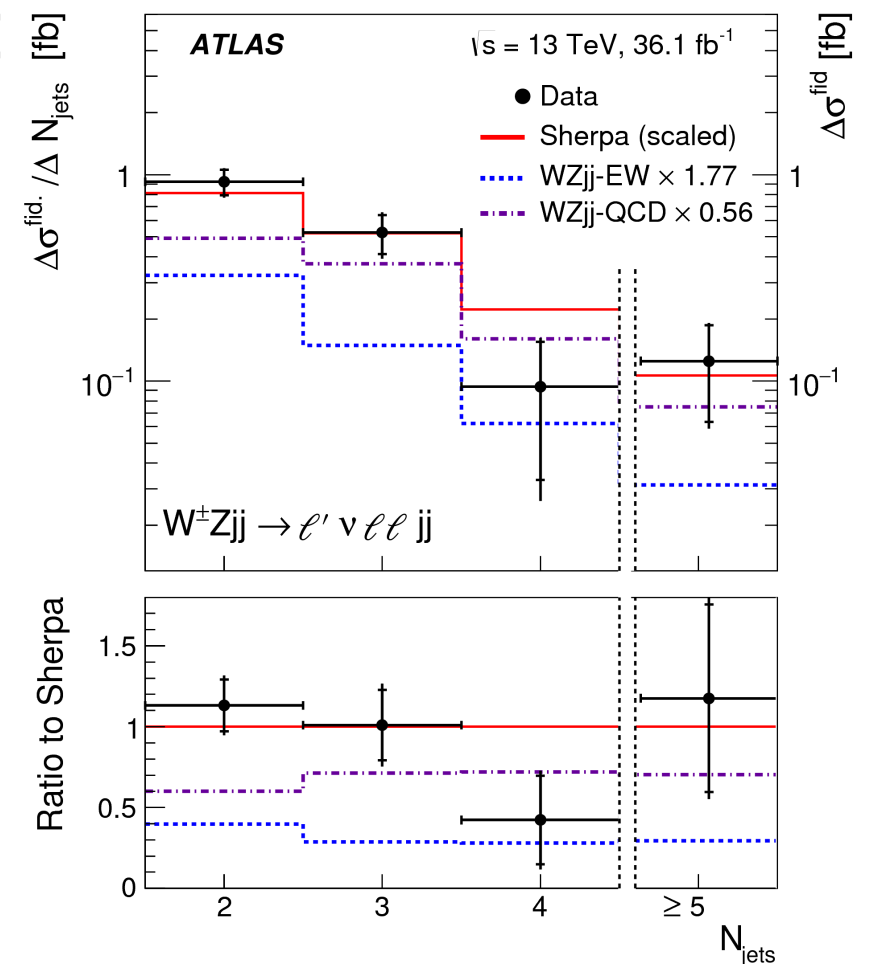
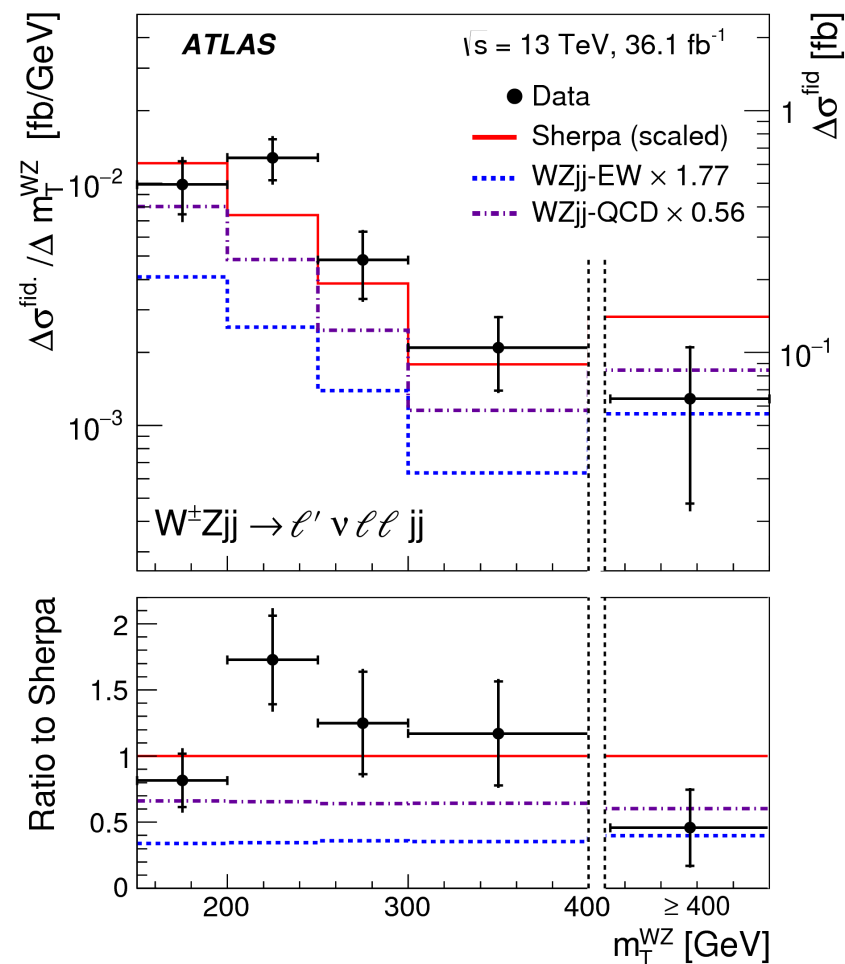
# WZ VBS

- ❖ 5.3 (3.20  $\sigma$ ) observed (exp.) significance.
- ❖ Fiducial cross-section for the electroweak production process (inc. interference with QCD process):  $0.57^{+0.14}_{-0.13}$  (stat.)  $^{+0.07}_{-0.06}$  (syst.) fb

- ❖ Sherpa under-predicts EW WZjj cross-section.

- ❖ Differential WZjj cross-section for  $\sum p_T^l$ ,

$$\Delta\phi(W, Z), m_T^{WZ}, N_{jets}, \Delta y_{jj}, m_{jj}, N_{jets}^{gap}, \Delta\phi_{jj}$$



---

# same-sign WW VBS

---

- ❖ Largest ratio of EW to QCD production cross-sections.
- ❖ Isolated well reconstructed same-sign dilepton events (e or  $\mu$ ).
- ❖ Veto third lepton to suppress WZ and veto b-jets to suppress tt.
- ❖ Fiducial region:
  - ❖ Same sign dilepton:  $p_T > 27$  GeV,  $|\eta| < 2.5$ ,  $m_{ll} > 20$  GeV,  $\Delta R(l, l) > 0.3$
  - ❖ vector sum of  $p_T$  of the two final state neutrinos  $p_T^{VV} > 30$  GeV
  - ❖ Two anti- $k_T$  0.4 jets with  $p_T > 65, 35$  GeV,  $|\eta| < 4.5$ ,  $m_{jj} > 500$  GeV,  $|\Delta y_{jj}| > 2$ ,  $\Delta R(j, l) > 0.3$
- ❖ Signal: Sherpa 2.2.2 WWjj

# same-sign WW VBS

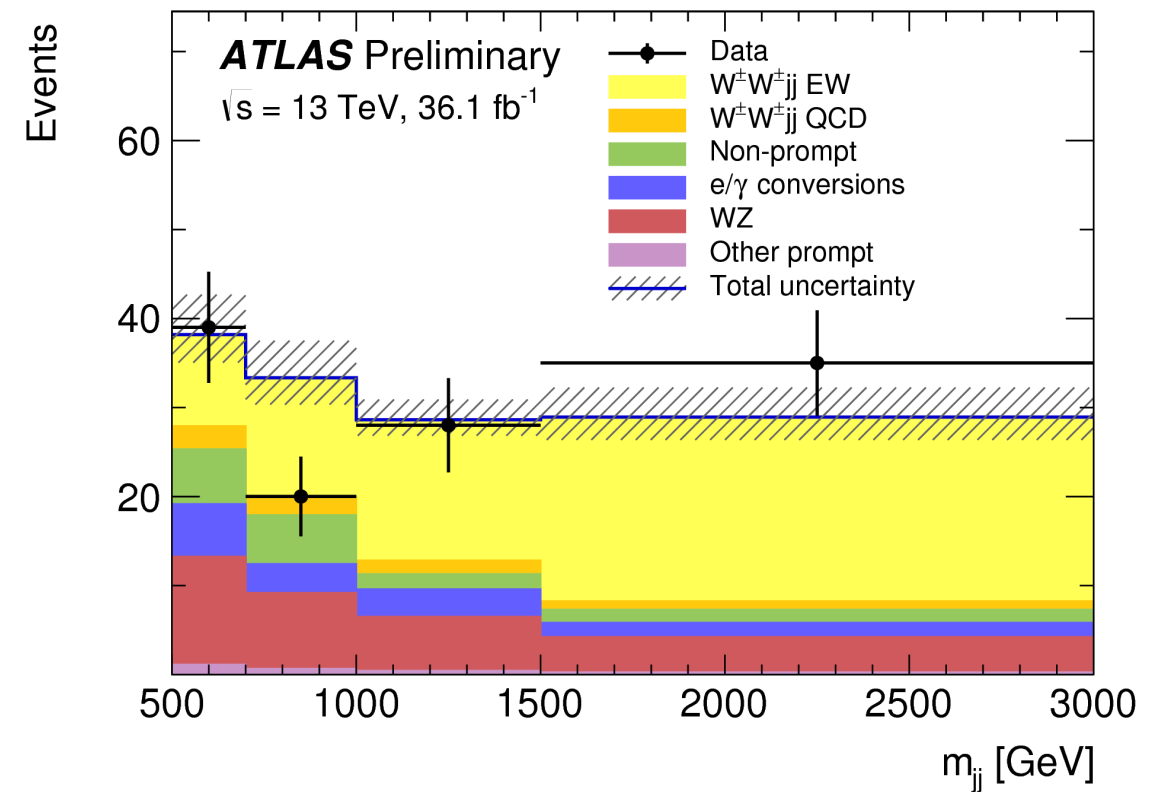
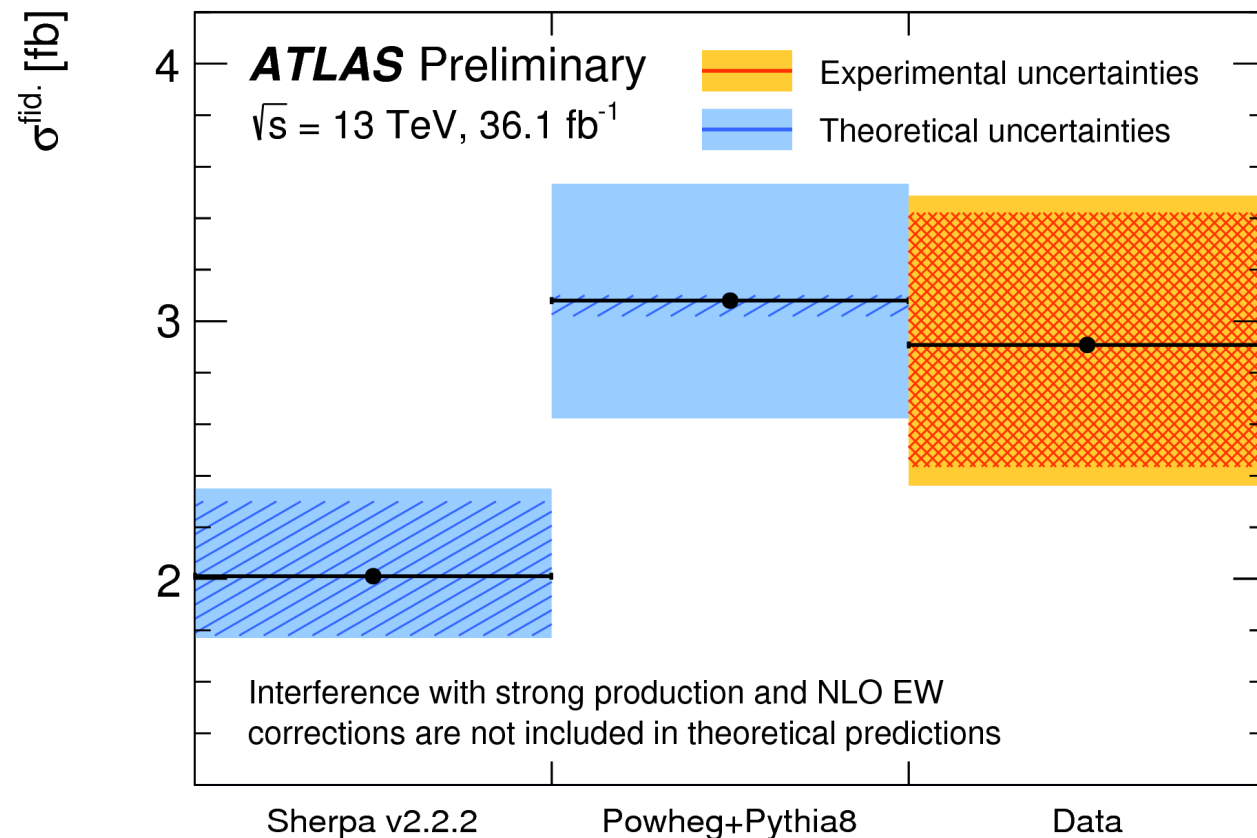
- ❖ Background: non-prompt lepton, charge mis-ID,  $V\gamma$ , ZZ, ttV, VVV, WZ.
  - ❖ Non-prompt lepton background measured from control regions with 40-90% uncertainty (Dominant experimental uncertainty)
- ❖ Likelihood fit:
  - ❖ Categorised into 6 channels:  $e^\pm e^\pm$ ,  $e^\pm \mu^\pm$ ,  $\mu^\pm \mu^\pm$ .
  - ❖ Signal region: 4  $m_{jj}$  bins for  $m_{jj} > 500\text{GeV}$ . Control region:  $200 < m_{jj} < 500\text{GeV}$ .

## Event yield before fit

	$e^+e^+$	$e^-e^-$	$e^+\mu^+$	$e^-\mu^-$	$\mu^+\mu^+$	$\mu^-\mu^-$	combined
WZ	$1.7 \pm 0.6$	$1.2 \pm 0.4$	$13 \pm 4$	$8.1 \pm 2.5$	$5.0 \pm 1.6$	$3.3 \pm 1.1$	$32 \pm 9$
Non-prompt	$4.1 \pm 2.4$	$2.3 \pm 1.8$	$9 \pm 6$	$6 \pm 4$	$0.57 \pm 0.16$	$0.67 \pm 0.26$	$23 \pm 12$
$e/\gamma$ conversions	$1.74 \pm 0.31$	$1.8 \pm 0.4$	$6.1 \pm 2.4$	$3.7 \pm 1.0$	-	-	$13.4 \pm 3.5$
Other prompt	$0.17 \pm 0.06$	$0.14 \pm 0.05$	$0.90 \pm 0.24$	$0.60 \pm 0.25$	$0.36 \pm 0.12$	$0.19 \pm 0.07$	$2.4 \pm 0.5$
$W^\pm W^\pm jj$ strong	$0.38 \pm 0.13$	$0.16 \pm 0.06$	$3.0 \pm 1.0$	$1.2 \pm 0.4$	$1.8 \pm 0.6$	$0.76 \pm 0.26$	$7.3 \pm 2.5$
Expected background	$8.1 \pm 2.4$	$5.6 \pm 1.9$	$32 \pm 7$	$20 \pm 5$	$7.7 \pm 1.7$	$4.9 \pm 1.1$	$78 \pm 15$
$W^\pm W^\pm jj$ electroweak	$3.80 \pm 0.30$	$1.49 \pm 0.13$	$16.5 \pm 1.2$	$6.5 \pm 0.5$	$9.1 \pm 0.7$	$3.50 \pm 0.29$	$40.9 \pm 2.9$
Data	10	4	44	28	25	11	122

# same-sign WW VBS

- ❖ Observed (expected) signal significance of 6.9 (4.6)  $\sigma$ .
- ❖ Modelling of this process studied in [ATL-PHYS-PUB-2019-004](#).



- ❖ Fiducial cross section for the electroweak production process (inc. interference):

$$2.91^{+0.51}_{-0.47} (\text{stat.}) \pm 0.27 (\text{sys.}) \text{ fb}$$

---

# Summary

---

- ❖ Presented 3 ATLAS results using  $36.1 \text{ fb}^{-1}$  of data at  $\sqrt{s} = 13 \text{ TeV}$ .
  - ❖ WZ production cross sections and polarisation
  - ❖ Observation of electroweak  $W^\pm Z jj$
  - ❖ Observation of electroweak same-sign  $W^\pm W^\pm jj$
- ❖ Helicity fractions of diboson measured first time in hadron collider.
- ❖ Vector boson scattering in WZ and same-sign WW has been observed with 5.3 and 6.9  $\sigma$ .
- ❖ Measurements agree with SM predictions so far.
- ❖ More diboson measurements coming soon, stay tuned.

Back-up slides

---

# Resonant shape algorithm

---

- ❖ Dressed leptons, and final-state neutrinos are matched to the W and Z boson decay products using a Monte Carlo generator-independent algorithm, called the “resonant shape” algorithm.

$$P = \left| \frac{1}{m_{(\ell^+, \ell^-)}^2 - (m_Z^{\text{PDG}})^2 + i \Gamma_Z^{\text{PDG}} m_Z^{\text{PDG}}} \right|^2 \times \left| \frac{1}{m_{(\ell', \nu_{\ell'})}^2 - (m_W^{\text{PDG}})^2 + i \Gamma_W^{\text{PDG}} m_W^{\text{PDG}}} \right|^2$$

- ❖ The final choice of which leptons are assigned to the W or Z bosons corresponds to the configuration exhibiting the largest value of the estimator.

---

# Transverse mass

---

$$m_T^W = \sqrt{2 \cdot p_T^\nu \cdot p_T^\ell \cdot [1 - \cos \Delta\phi(\ell, \nu)]}$$

- ❖  $p_T^\nu$  at detector level computed using  $E_T^{\text{miss}}$ .

$$m_T^{WZ} = \sqrt{\left(\sum_{\ell=1}^3 p_T^\ell + E_T^{\text{miss}}\right)^2 - \left[\left(\sum_{\ell=1}^3 p_x^\ell + E_x^{\text{miss}}\right)^2 + \left(\sum_{\ell=1}^3 p_y^\ell + E_y^{\text{miss}}\right)^2\right]}$$

---

# Neutrino $p_z$ from $W$ mass constraint

---

- ❖  $W^\pm$  boson mass constraint is used to solve for the  $z$  component  $p_z^\nu$  of the neutrino momentum. This generally leaves a two-fold ambiguity which is resolved by choosing the solution with the smaller  $|p_z^\nu|$ .
- ❖ If the measured transverse mass is larger than the nominal  $W^\pm$  mass, no real solutions exist for  $p_z^\nu$ . The most likely cause is that the measured  $E_T^{\text{miss}}$  is larger than the actual neutrino  $p_T$ . In this case, the best estimate is obtained by choosing the real part of the complex solutions with the smaller magnitude.

# BDT

- ❖ Used to separate  $WZjj$ -EW signal and the  $WZjj$ -QCD and other backgrounds.
- ❖ 15 variables:
  - ❖ jet-kinematic variables:  $m_{jj}$ ,  $p_{T}^{j1}$ ,  $p_{T}^{j2}$ ,  $\Delta\eta_{jj}$ ,  $\Delta\phi_{jj}$ ,  $y_{j1}$ ,  $N_{jets}$
  - ❖ vector-bosons-kinematics variables:  $p_{T}^W$ ,  $p_{T}^Z$ ,  $\eta_w$ ,  $|y_Z - y_{l,wl}|$ ,  $m_{T}^{WZ}$
  - ❖ variables related to jets and leptons kinematics:  $\Delta R(j1, Z)$ , event balance  $R_{p_{T}^{hard}}$ , centrality of WZ system relative to the tagging jets
- ❖ The good modelling by MC simulations of the distribution shapes and the correlations of all input variables to the BDT is verified in the  $WZjj$ -QCD CR
- ❖  $R_{p_{T}^{hard}}$  : transverse component of the vector sum of the WZ bosons and tagging jets momenta, normalised to their scalar  $p_T$  sum,

